







RESEARCH ARTICLE | JULY 06 2023

Power scaling of a self-mode-locked vertical-external-cavity surface-emitting laser

Ri Yan ; Renjiang Zhu ; Yadong Wu ; Tao Wang; Lidan Jiang; Huanyu Lu; Yanrong Song ; Peng Zhang  

 Check for updates

Appl. Phys. Lett. 123, 011106 (2023)

<https://doi.org/10.1063/5.0154291>



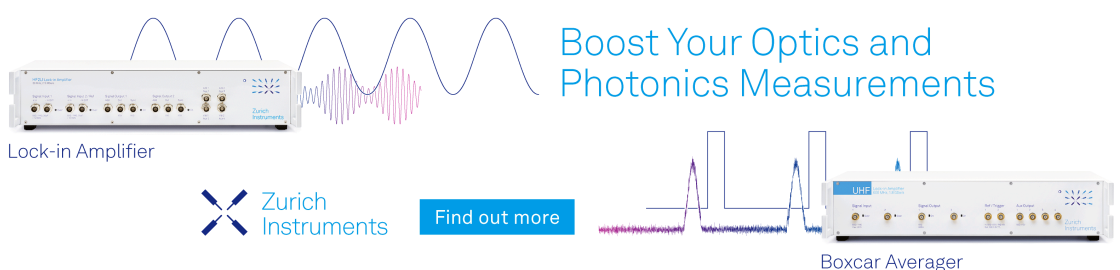
View Online




Export Citation

CrossMark

Boost Your Optics and Photonics Measurements



Lock-in Amplifier

 Zurich Instruments

[Find out more](#)

Boxcar Averager

Power scaling of a self-mode-locked vertical-external-cavity surface-emitting laser

Cite as: Appl. Phys. Lett. **123**, 011106 (2023); doi: [10.1063/5.0154291](https://doi.org/10.1063/5.0154291)

Submitted: 13 April 2023 · Accepted: 19 June 2023 ·

Published Online: 6 July 2023



View Online



Export Citation



CrossMark

Ri Yan,¹  Renjiang Zhu,^{1,a)}  Yadong Wu,¹  Tao Wang,¹  Lidan Jiang,¹  Huanyu Lu,²  Yanrong Song,³  and Peng Zhang^{4,a)} 

AFFILIATIONS

¹College of Physics and Electronic Engineering, Chongqing Normal University, Chongqing 401331, China

²Changchun Institute of Optics, Fine Mechanics and Physics, Chinese Academy of Sciences, Jilin 130033, China

³College of Applied Sciences, Beijing University of Technology, Beijing 100124, China

⁴National Center for Applied Mathematics in Chongqing, Chongqing Normal University, Chongqing 401331, China

^{a)}Authors to whom correspondence should be addressed: 20131121@cqnu.edu.cn and zhangpeng2010@cqnu.edu.cn

ABSTRACT

A typical self-mode-locked vertical-external-cavity surface-emitting laser must operate at the edge of the stable region of the resonant cavity. Its minimal pump spot on the gain chip is used as a soft aperture. By comparing with a continuous-wave (CW) laser, the pulsed laser is focused more tightly on the gain chip due to the Kerr-lens effect. This mitigates cavity loss of the pulsed laser in comparison with the CW laser, such that successive mode-locking can be initiated. The disadvantage of the above method is that the relatively small pump spot, producing relatively large thermal effect, limits the output power of the laser. To address this issue, we propose another method with the work point of the laser moved slightly from the edge of the stable region and the pump spot moderately extended, with a spot of the pulsed laser on the gain chip that could be smaller or larger than that of the CW laser. We achieve stable self-mode-locking with a record average output power of 8.18 W in a V-type resonator, limited by the applied pump power. The pulse repetition rate and width are 0.71 GHz and 1.92 ps, respectively, and the corresponding peak power is 5.6 kW.

Published under an exclusive license by AIP Publishing. <https://doi.org/10.1063/5.0154291>

The vertical-external-cavity surface-emitting laser (VECSEL) combines the advantages of optically pumped solid-state and semiconductor lasers,^{1–3} offering a broad range of emission wavelengths, excellent beam quality, and high output power. Furthermore, its external cavity facilitates the insertion of other optical components for wavelength tuning, frequency converting, linewidth narrowing, etc.^{4–6}

In a VECSEL, mode-locking is achieved by employing a saturable absorber, such as the semiconductor saturable absorption mirror (SESAM).⁷ In a SESAM mode-locked VECSEL, the laser beam must be tightly focused on the SESAM to ensure that it saturates before the gain medium, enabling build-up of the mode-locking. In this case, a serious thermal effect is unavoidable, and the output power of the laser is limited. To date, the highest achieved power of a SESAM mode-locked VECSEL was 5.1 W.⁸

Mode-locking can also be realized in a VECSEL by using the Kerr effect in the active region of the gain chip, which is also referred to as self-mode-locking.^{9,10} By comparing with the SESAM mode-locked VECSEL, a self-mode-locked (SML) VECSEL requires no additional saturable absorber in the cavity, and the laser becomes more compact and more cost-effective and has less limitations.

After constructing the first SML VECSEL with a 654 fs pulse width, a 0.45 W average output power and 2.17 GHz repetition rate were reported by Chen *et al.* in 2011.¹¹ Kornaszewski *et al.* reported an SML VECSEL with an output power of 700 mW and a pulse duration of 1.5 ps at a 200 MHz repetition rate.¹² In their study, the origin of mode-locking was first attributed to an intensity-dependent Kerr-lens generated in the semiconductor gain medium. Later, Albrecht *et al.* analytically predicted Kerr-lens mode-locking and experimentally verified it. An average output power of about 1.1 W with a 500 fs pulse width at a 1 GHz repetition rate was obtained.¹³

Gaafar *et al.* provided clear evidence of mode-locking in an SML VECSEL using nonlinear frequency conversion and long-time-span autocorrelation measurements.¹⁴ They also demonstrated an SML VECSEL in the fundamental and higher harmonic mode-locking¹⁵ and a quantum dot gain chip-based SML VECSEL.¹⁶ Furthermore, self-mode-locking in an AlGaInP-based 666 nm VECSEL was achieved by Bek *et al.*¹⁷ and a dual-wavelength SML VECSEL was reported by Shen *et al.* in 2022.¹⁸

In the above-mentioned previously reported SML VECSELs, the laser was forced to work at the edge of the stable region of the resonant

cavity, and a so-called soft aperture was introduced by using the pump spot on the gain chip. In this case, the spot generated by the continuous-wave (CW) laser on the gain chip would be significantly larger than the pump spot. In contrast, owing to the Kerr-lens in the active region of the gain chip, the pulsed laser could better focus on the gain chip and suffer smaller cavity loss. In this way, mode-locking could be initiated. However, the small spot formed by the tight focusing of the pulsed laser, along with the smaller pump spot, results in serious thermal effects and limits the output power of the laser to a certain degree.

Here, we propose another method, where the work point of the laser is slightly drifted away from the edge of the stable region, and the pump spot is moderately extended. The length of each arm of the cavity can be carefully selected, such that the spot of the pulsed laser on the gain chip is smaller (or larger) than that of the CW laser. Meanwhile, the loss (or gain) difference between the CW and pulsed laser is designed to be a reasonable value such that the mode-locking can be initiated. Using this method, we achieved an average output power over 8 W under stable mode-locking in a simple V-type resonant cavity, and the laser has not yet experienced the thermal rollover.

The gain chip used in our experiment was epitaxially grown in reverse sequences, as shown in Fig. 1(a): the AlGaAs etch stop layer with high Al composition; the GaAs protective layer; the AlGaAs window layer with a high barrier, the active region, and the distributed Bragg reflector (DBR); and the antioxidant GaAs cap layer. There are 15 InGaAs/GaAsP quantum wells in the active region, and the content of In in the InGaAs well layer is designed to meet the target laser wavelength of 980 nm. The content of P in the GaAsP barrier layer (which also works as the strain compensation layer) must be adequate to compensate for the strain, but not excessive to absorb the pumping energy. The DBR is composed of 30 pairs of alternate AlGaAs layers with high Al (lower refractive index) and low Al (higher refractive index) composition. Its designed center wavelength and high-reflectivity bandwidth are 980 and 100 nm, respectively.

When the grown wafer is split to small chips of 4×4 mm dimension, the epitaxial end face is sequentially metalized with titanium-platinum-gold, after which the chip is bonded to a copper heatsink, and the substrate is removed using a chemical etch. The heatsink is mounted to a thermal-electronic cooler, which is then connected with a water-cooling system.

The V-type resonant cavity is shown in Figs. 1(a) and 1(b). The folded flat-concave mirror M1 with a 200 mm radius of curvature is high-reflectivity coated for the 980 nm wavelength, and a flat mirror M2 with 3% transmission is used as the output coupler. The angle of two arms of the resonant cavity L1 and L2 is approximately 12° . An 808 nm fiber-coupled semiconductor laser is collimated and focused on the gain chip at an incident angle of about 30° . The diameter of the pump spot on the gain chip is about $400 \mu\text{m}$.

In the below experiment, the autocorrelation trace is measured using a Femtochrome FR-103XL autocorrelator with >4 Hz repetition rate, >175 ps scan range, and <5 fs resolution. The laser spectrum is recorded by a HORIBA iHR320 spectrometer with a wavelength range of 150–1500 nm and a resolution of 0.006 nm. The mode-locked laser pulses are detected using a Thorlabs DET08C high-speed detector with a bandwidth of 6 GHz and a wavelength range of 800–1700 nm and recorded by a Tektronix MSO68B oscilloscope with a 10 GHz bandwidth and a 50 Gs/s sampling rate. A Rigol DSA800 radio frequency (RF) spectrum analyzer with a 7.5 GHz bandwidth and a 100 Hz–1 MHz resolution is employed to measure the repetition rate of the mode-locked pulse trains. The beam quality is measured by a Thorlabs M2MS BC106N beam quality analyzer with 350–1100 nm wavelength range, and the output power of the laser is obtained from an Ophir 12A-P detector and a NOVA II power meter.

As shown in Fig. 2, two different methods are employed to initiate the self-mode-locking. Method 1, the work point of the laser is chosen at the “A” point, which is lightly drifted away from the edge of the stable region of the laser cavity, as shown in Fig. 2(c1). The lengths of the two arms of the cavity are $L1 \approx 90$ and $L2 \approx 96$ mm. The evolution of the mode size in the cavity is plotted in Fig. 2(a1), and the corresponding spot sizes of the CW and pulsed laser on the gain chip are $\omega_{\text{CW}} \approx 222$ and $\omega_{\text{ML}} \approx 174 \mu\text{m}$, respectively. The focal distance of the Kerr-lens use in the above computation is estimated by $f_{\text{Kerr}} \approx a\pi\omega^4 / (8n_2 P_{\text{peak}} L)$.¹⁴ Parameter a can be chosen between 4 to 6 (we use 4 in this study), and the typical value of the nonlinear refractive index is $n_2 \approx -10^{-12} \text{ cm}^2/\text{W}$. The radius of the laser spot and the thickness of the Kerr medium are chosen to be $\omega \approx 200$ and $L \approx 3.5 \mu\text{m}$ (i.e., the thickness of the active region in the gain chip), respectively. The peak power of the pulsed laser in the resonant cavity is $P_{\text{peak}} = P / (f_{\text{rep}} \Delta t_p)$, and the average output power, pulse repetition rate, and pulse width are all selected to be close to their typical values (which means also

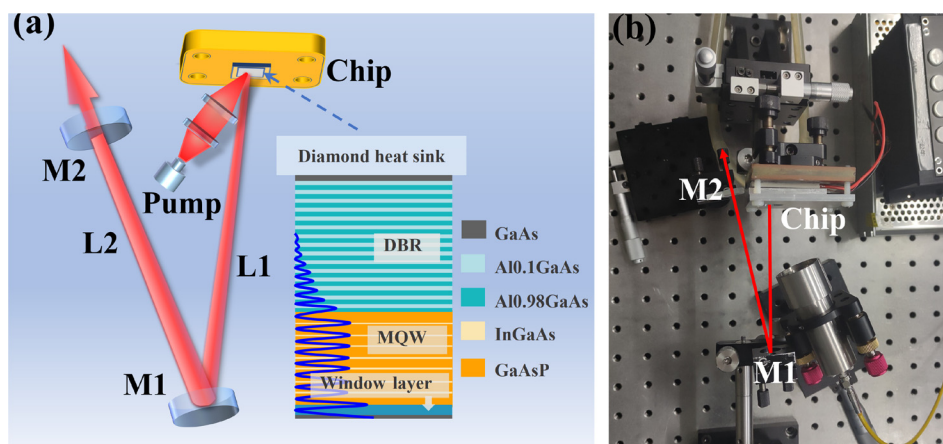


FIG. 1. Schematics of SML VECSEL (a) and top view of experimental setup (b). The inset in the lower right corner in (a) depicts the epitaxial structure of the gain chip.

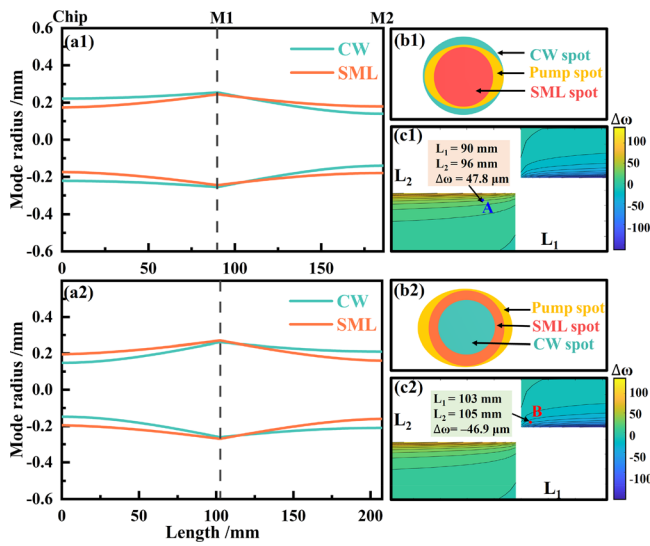


FIG. 2. (a1) and (a2) Calculated evolution of mode sizes of CW and pulsed lasers in the cavity. (b1) and (b2) Relationship between the spots of the pump, CW, and pulsed laser on the gain chip. (c1) and (c2) Work point in the stable region of the resonant cavity of the SML VECSEL. Subscripts 1 and 2 correspond to the two methods employed in the experiment.

close to our experiment). These are $P \approx 4$ W (3% transmission), $f_{\text{rep}} \approx 600$ MHz, $\Delta t_p \approx 2$ ps. Hence, the circulating peak power inside the cavity is calculated to be $P_{\text{peak}} \approx 110$ kW, and as a result, the focal length of the Kerr-lens is about $f_{\text{kerr}} \approx -3000$ mm.

Under these conditions, the relationship between the pump spot, CW laser, and pulsed laser spots on the gain chip is illustrated in Fig. 2(b1). For the CW laser, the pump spot works as an aperture, which makes it suffer additional losses. For the pulsed laser, because of Kerr-lens, under the condition of $L_1 \approx 90$ and $L_2 \approx 96$ mm, the laser spot is smaller than the pump spot, and the calculated difference of the spot radius between the CW and pulsed laser is $\Delta\omega = \omega_{\text{CW}} - \omega_{\text{ML}} \approx 48$ μm . Considering that the angle between L_1 and L_2 is not zero (e.g., 12° in our experiment), the tangential and sagittal focus lengths of M1 are $f_t = f \cdot \cos \theta$ and $f_s = f / \cos \theta$, respectively. Replacing the focal length f used in Fig. 2 with the focal lengths f_t and f_s , results show that the difference between the recalculated and the original $\Delta\omega$ is about 2%. Thus, the relatively small angle does not significantly affect the build-up of mode-locking and the output power of mode-locked laser in this experiment.

By using $\Delta\omega \approx 48$ μm and integrating the Gaussian spot, we can compute the additional loss experienced by the CW laser at about 3% compared to the pulsed laser. It is this additional loss that suppresses the CW laser, starts the mode-locking, and maintains the stable operation of the pulsed laser.

The selection of $\Delta\omega$ follows the rules listed below. First, to achieve good mode-matching during the mode-locked operation, thus effectively improving the power of the mode-locked laser, the size of the pulsed laser spot must be as close as possible to the pump spot. Second, $\Delta\omega$ must be large enough to make the cavity loss or gain of the CW laser significantly higher or lower than that of the pulsed laser, respectively, hence, to initiate the mode-locking. Third, if $\Delta\omega$ is excessively large, it will cause the laser and pump spots to deviate

significantly from the mode-matching of CW operation, making it difficult for the laser to oscillate. Therefore, $\Delta\omega$ must assume a compromised value. In our experiment, the maximum output power was achieved when $\Delta\omega$ was about 12% of the pump spot diameter (400 μm).

Figure 3(a1) shows the mode-locked pulse train, and the inset indicates the uniformity of mode-locked pulses over a microsecond time extension. Figure 3(b1) depicts the measured repetition rate of SML laser pulses. The RF signal strength exceeds 60 dB, and the repetition rate of 0.81 GHz corresponds to the cavity length of 186 mm. The inset in the upper-right corner includes the higher-order harmonics of the repetition rate, whose rapid attenuation is caused by the bandwidth limitation (7.5 GHz) of the RF spectrum analyzer employed in the experiment. The output power of the SML laser is shown in Fig. 4. When the pump power is 35 W, the obtained maximum output power is 4.86 W, and the slope efficiency is 16.8%. The maximum output power of the SML laser is limited by our pump source. To date, the laser has not experienced thermal rollover and is still stably mode-locked.

Method 2, the work point of the laser is chosen at the “B” point, as shown in Fig. 2(c2). The lengths of the two arms of the cavity are $L_1 \approx 103$ and $L_2 \approx 105$ mm. The evolution of the mode size in the cavity is plotted in Fig. 2(a2), and the corresponding spot sizes of the CW and pulsed laser on the gain chip are 148 and 195 μm , respectively.

The relationship between the pump, CW laser, and pulsed laser spots is shown in Fig. 2(b2) for the laser working at the “B” point. In this case, the lengths of L_1 and L_2 are carefully selected such that the spots of the CW and pulsed laser on the gain chip are all smaller than the pump spot. Among them, the CW laser spot is suppressed to be the smallest one, while the spot size of the pulsed laser is pushed as close to the pump spot as possible. When the two arms of the cavity are $L_1 \approx 103$ and $L_2 \approx 105$ mm, the radius difference between the spots of the CW and the pulsed laser is about $\Delta\omega = \omega_{\text{CW}} - \omega_{\text{ML}} \approx -47$ μm . The pulsed light is estimated to obtain approximately 10% more gain from the pump than the CW light. This larger gain enables the pulsed laser to win in the mode competition and plays a crucial role in the initiation of the mode-locking.

The mode-locked pulse train is presented in Fig. 3(a2), and the inset in the upper-right corner over a microsecond indicates a consistent amplitude and the absence of a modulation envelope, demonstrating stable mode-locking. Figure 3(b2) describes the repetition rate of mode-locked pulses, and the evident peak at 0.71 GHz matches the 208 mm cavity length of the SML VECSEL. The inset depicts the RF spectrum of the first seven harmonics within a 5 GHz range. The absence of other beat frequency signals indicates good stability and continuity of mode-locking.

The autocorrelation measurement of SML pulses is shown in Fig. 3(c2). The full width at half maximum (FWHM) of the Gaussian fit is 1.93 ps. Figure 3(d2) shows the mode-locked laser spectrum with an FWHM of 1.36 nm. The time-bandwidth product of the mode-locked pulse is 0.819, nearly twice the value (0.441) of the Fourier-transform limit of an ideal Gaussian pulse. This suggests that there is evident chirp in the mode-locked pulse, which may result from the nonlinear refractive index in the active region of the gain chip.

The output power with respect to the absorbed pump power of the SML laser is plotted in Fig. 4. The maximum output power of 8.18 W is achieved when the pump power is 35 W, and the slope efficiency is 25.2%. The maximum output power is limited by our pump

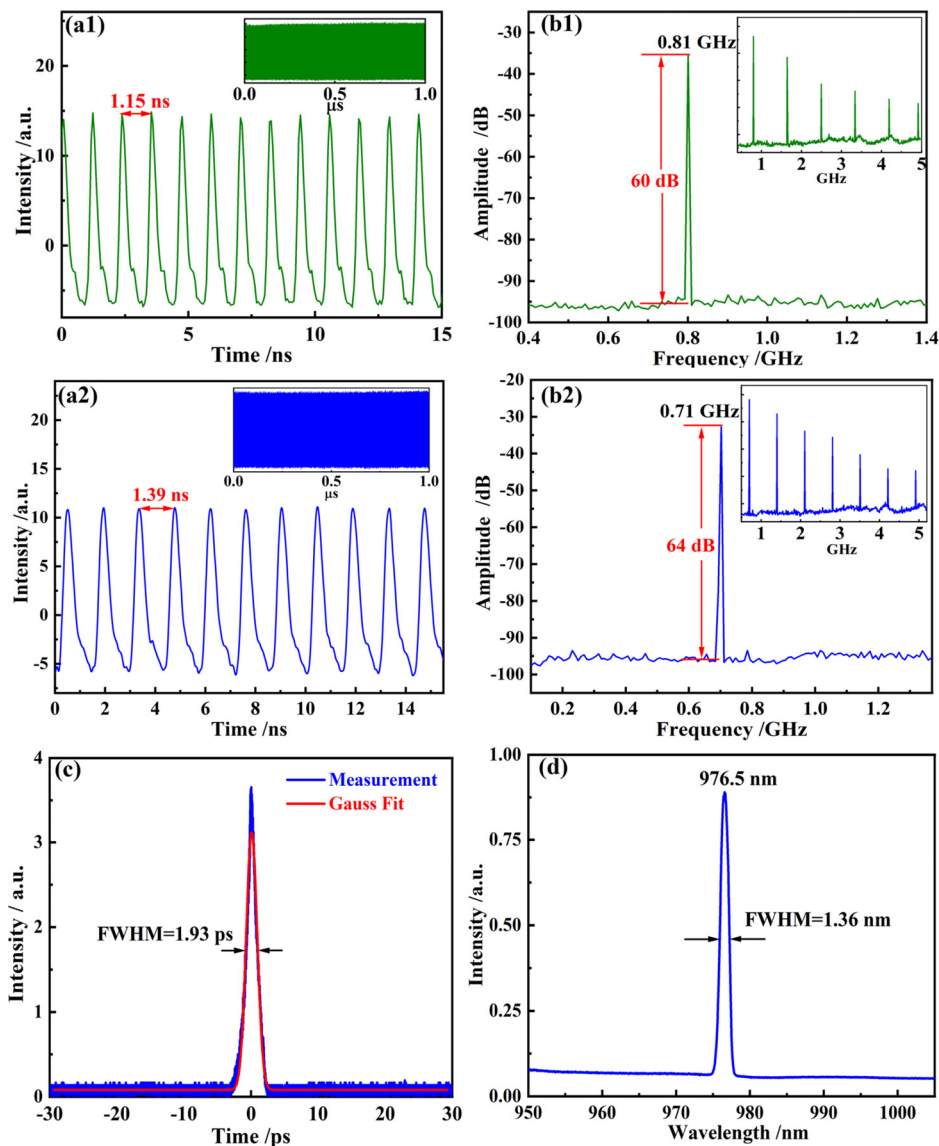


FIG. 3. (a1) and (a2) Pulse train of SML VECSEL. (b1) and (b2) RF spectrum of repetition rate of the mode-locked laser with a 10 kHz resolution bandwidth. (c) Autocorrelation trace of SML pulses and (d) laser spectrum centered at 976.5 nm. Insets in (a1) and (a2) show the pulse train in microsecond time extension, while insets in (b1) and (b2) indicate higher-harmonics of the repetition rate of SML pulses.

source, and the laser is stable with steady mode-locking and without thermal rollover.

The measured beam quality factor M^2 is plotted in the inset of Fig. 4, and the values of 1.04 in the x -direction and 1.03 in the y -direction indicate a near-diffraction-limited Gaussian beam. The two-dimensional distribution of the light intensity is also given.

By comparing with the commonly used approach for soft-aperture-started self-mode-locking (where the pump laser has the smallest spot on the Kerr medium, while the pulsed laser is focused tightly and is closer to the pump spot than the CW laser), the strategy of expanding the pump spot employed in this article holds evident advantages in improving the output power of an SML VECSEL. Owing to the significant reduction of the thermal effect of the laser for both methods described in this paper, the lasers all have not yet experienced thermal rollover while maintaining steady mode-locking. In Fig. 4, the

maximum average output power and slope efficiency obtained using method 2 are significantly higher than those obtained using method 1. The reason is that the spot of the pulsed laser in method 2 is larger and more similar to the pump spot, which is superior to method 1 in terms of reducing the thermal effects and improving pump utilization. Thus, method 2 is preferred, because the mode difference between the CW and pulsed lasers is greater than in method 1, and because the resonant cavity has stronger ability to distinguish modes, such that the laser maintains a relatively stable mode-locking at a higher power level.

In summary, we demonstrated the power scaling of an SML VECSEL by moderately extending the pump spot and carefully designing the mode size of the CW and pulsed laser on the gain chip. Mode-locking can be initiated by the loss difference between the CW light with a spot larger than the pump and the pulsed laser with a spot smaller than the pump. This mode-locking can also be initiated by the

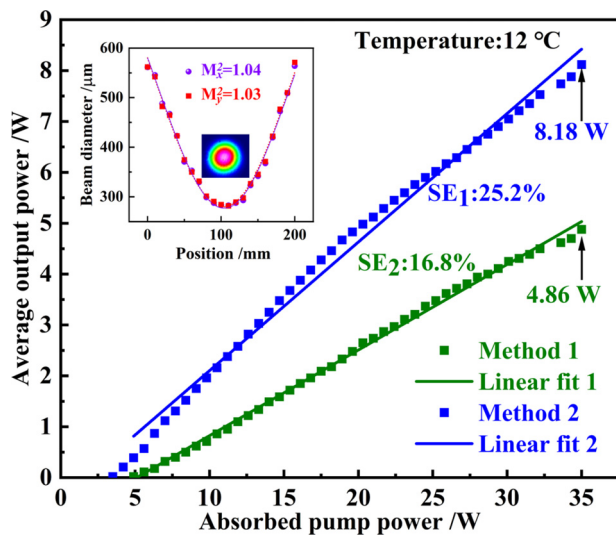


FIG. 4. Average output power with respect to absorbed pump power of the stable SML VECSEL. The inset describes the beam quality factor M^2 in x - and y -directions and the 2D distribution of the light intensity of the SML laser beam.

gain difference between the CW laser with the smallest spot and the pulsed laser with a spot larger than the CW but smaller than the pump. In the second method, stable self-mode-locking with a slope efficiency of 25.2% and a record average output power of 8.18 W, which is limited by the used pump power, is achieved in a V-type resonator. The pulse repetition rate is 0.71 GHz, the pulse width is 1.92 ps, and the corresponding peak power of the laser pulse is 5.6 kW.

This work was supported by the Cooperation Project between Chongqing Local Universities and Institutions of Chinese Academy of Sciences, Chongqing Municipal Education Commission (No. HZ2021007), the Science and Technology Research Program of Chongqing Municipal Education Commission (No. KJZD-M201900502), the Science and Technology Research Program of Chongqing Municipal Education Commission (No. KJQN202200557), and the National Natural Science Foundation of China (Nos. 61975003, 61790584, and 62025506).

AUTHOR DECLARATIONS

Conflict of Interest

The authors have no conflicts to disclose.

Author Contributions

Ri Yan: Formal analysis (equal); Investigation (equal); Methodology (equal); Resources (equal); Validation (equal); Visualization (equal);

Writing – original draft (equal); Writing – review & editing (equal). **Renjiang Zhu:** Formal analysis (equal); Investigation (equal); Visualization (equal); Writing – review & editing (equal). **Yadong Wu:** Formal analysis (supporting); Investigation (supporting); Resources (equal); Validation (supporting). **Tao Wang:** Formal analysis (supporting); Funding acquisition (supporting); Investigation (supporting); Validation (supporting). **Lidan Jiang:** Formal analysis (supporting); Validation (supporting). **HuanYu Lu:** Investigation (supporting); Resources (supporting). **Yanrong Song:** Formal analysis (supporting); Writing – review & editing (supporting). **Peng Zhang:** Conceptualization (lead); Funding acquisition (lead); Methodology (equal); Project administration (lead); Supervision (lead).

DATA AVAILABILITY

The data that support the findings of this study are available from the corresponding authors upon reasonable request.

REFERENCES

- ¹M. Guina, A. Rantamäki, and A. Härkönen, *J. Phys. D* **50**, 383001 (2017).
- ²A. Rahimi-Iman, *J. Opt.* **18**, 093003 (2016).
- ³M. Kuznetsov, F. Hakimi, R. Sprague, and A. Mooradian, *IEEE Photonics Technol. Lett.* **9**, 1063 (1997).
- ⁴O. Castany, L. Dupont, A. Shuaib, J. P. Gauthier, C. Levallois, and C. Paranthoën, *Appl. Phys. Lett.* **98**, 161105 (2011).
- ⁵O. Casel, D. Woll, M. A. Tremont, H. Fuchs, R. Wallenstein, E. Gerster, P. Unger, M. Zorn, and M. Weyers, *Appl. Phys. B* **81**, 443 (2005).
- ⁶B. Heinen, T.-L. Wang, M. Sparenberg, A. Weber, B. Kunert, J. Hader, S. W. Koch, J. V. Moloney, M. Koch, and W. Stolz, *Electron. Lett.* **48**, 516 (2012).
- ⁷S. Hoogland, S. Dhanjal, A. C. Tropper, J. S. Roberts, R. Häring, R. Paschotta, F. Morier-Genoud, and U. Keller, *IEEE Photonics Technol. Lett.* **12**, 1135 (2000).
- ⁸M. Scheller, T.-L. Wang, B. Kunert, W. Stolz, S. W. Koch, and J. V. Moloney, *Electron. Lett.* **48**, 588 (2012).
- ⁹M. A. Gaafar, A. Rahimi-Iman, K. A. Fedorova, W. Stolz, E. U. Rafailov, and M. Koch, *Adv. Opt. Photonics* **8**, 370 (2016).
- ¹⁰U. Keller and A. C. Tropper, *Phys. Rep.* **429**, 67 (2006).
- ¹¹Y. Chen, Y. Lee, H. C. Liang, K. Y. Lin, K. Su, and K. F. Huang, *Opt. Lett.* **36**, 4581 (2011).
- ¹²L. Kornaszewski, G. Maker, G. P. A. Malcolm, M. Butkus, E. U. Rafailov, and C. J. Hamilton, *Laser Photonics Rev.* **6**, L20 (2012).
- ¹³A. R. Albrecht, Y. Wang, M. Ghasemkhani, D. V. Seletskiy, J. G. Cederberg, and M. Sheik-Bahae, *Opt. Express* **21**, 28801 (2013).
- ¹⁴M. Gaafar, P. Richter, H. Keskin, C. Möller, M. Wichmann, W. Stolz, A. Rahimi-Iman, and M. Koch, *Opt. Express* **22**, 28390 (2014).
- ¹⁵M. Gaafar, C. Möller, M. Wichmann, B. Heinen, B. Kunert, A. Rahimi-Iman, W. Stolz, and M. Koch, *Electron. Lett.* **50**, 542 (2014).
- ¹⁶M. Gaafar, D. A. Nakdali, C. Möller, K. Fedorova, M. Wichmann, M. Shakfa, F. Zhang, A. Rahimi-Iman, E. Rafailov, and M. Koch, *Opt. Lett.* **39**, 4623 (2014).
- ¹⁷R. Bek, M. Grossmann, H. Kahle, M. Koch, A. Rahimi-Iman, M. Jetter, and P. Michler, *Appl. Phys. Lett.* **111**, 182105 (2017).
- ¹⁸X.-H. Shen, Y.-Y. Zeng, L. Mao, R.-J. Zhu, T. Wang, H.-J. Luo, C.-Z. Tong, J.-W. Li, Y.-R. Song, and P. Zhang, *Acta Phys. Sin.* **71**, 88 (2022).